JOURNAL OF SPACECRAFT AND ROCKETS
Vol. 46, No. 1, January–February 2009

Durability of Polymeric Materials in Space: Application of Scanning Thermal Microscopy

Hartmut Fischer*
TNO Science and Technology, 5600 HE Eindhoven, The Netherlands
Delft University of Technology, 2629 HS Delft, The Netherlands
and
Christopher O. A. Semprimoschnig†
ESA, 2200 AG Noordwijk, The Netherlands

DOI: 10.2514/1.33362

In this work, a new method, the scanning thermal microscopy method, is applied to study the durability of polymeric materials for space applications. The method was applied to study ground-tested as well as space-retrieved materials. Space-grade silicones, high-temperature polyimides, and the well-known second-surface-mirror-material, fluorinated ethylene propylene, were analyzed as materials. It is shown that the method is particularly suitable for the fluorinated ethylene propylene material, and subtle differences of the top surface layer caused by different exposure conditions (solar ultraviolet, vacuum ultraviolet radiation, thermal aging, etc.) can be revealed. The technique proves to be very suitable for the study of the surface-degradation effects of materials exposed to space as well as to a simulated space environment.

I. Introduction

MICROTHERMAL analysis, a combination of the established knowledge in thermal analysis and of the scanning probe microscopy, was successfully introduced to the public during the Pittsburgh Conference (PitCon 1998) [1]. Since then, the method to inspect surfaces with respect to their thermal properties by using a scanner with a thermal sensor as the probe (tip) has been explored and tested on many different materials and surfaces [1–3]. The scanning thermal microscope (SThM) system combines the visualization power of atomic force microscopy and its ability to image topography, phase shifts, friction, stiffness, and adhesion with the characterization capabilities of thermal analysis (thermal conductivity, microdifferential thermal analysis, and microthermomechanical analysis) in a single instrument. This gives new insight into the physical and chemical structure of the surface of a material. It surpasses mere topographical mapping (commonly used in atomic force microscopy imaging) because heat flow differences can be correlated to differences in chemical or physical structure. During scanning at elevated temperatures, tiny differences in heat conductivity of the material(s) under inspection can be visualized. The highest sensitivity is present in the low- and medium-λ range (differences of 0.05 W/mK can be resolved); the lateral resolution in topology is about 1 μm, in the thermal mode it is up to 60 nm, and in the horizontal resolution, it is approximately 2 nm.

A simultaneous registration of topology and thermal properties (conductivity or diffusivity) gives unique possibilities to spot differences in material (polymers, metals, and ceramics) phases and even to reveal defects/changes below the surface. Spots of interest may be analyzed using the local thermal analysis (LTA) mode. Here, the tip is brought in contact with the material and heated up (heating rate up to 1200 K/ minwith a range up to 900°C). The heat flow to the sample (calorimetric signal) and the sensor location (thermomechanical signal) is registered to detect useful phase transformations for identification of materials and changes (damages) at the surfaces of materials. Any thermodynamic phase transition connected with a change in mechanical properties (softening, expansion, melting) and thermal properties (heat of fusion and change of heat capacity) will thus be detected by both methods. Therefore, a thermal image of the chemical or physical structure of the surface and the underlying material can be obtained. This enables, for instance, studying changes in molecular weight and cross-link density of polymers on surfaces as well as an in-depth study of such phenomena. This may even be used for quantitative analysis of polymeric materials, for thickness analysis of thin layers, etc. Interesting applications are, for example, mapping of differences in T_g of copolymers or the determination of chain scission due to irradiation damage.

The aim of this study is to perform exploratory investigations and to evaluate the capabilities of the SThM techniques for detection and understanding of degradation phenomena and mechanisms of polymeric materials exposed to extended space environmental ground simulation by radiation, thermal cycling, and thermal aging. In addition, space-retrieved materials were analyzed and the effects of the space environment were studied. For the investigations, the scanning mode and, in particular, the local thermal analysis mode were mainly employed.

The study concentrates on space environmentally ground-tested materials [e.g., irradiated and thermally aged silicones, polyimides, and fluorinated ethylene propylene (FEP)] as well as on space-retrieved FEP coming from the Long Duration Exposure Facility (LDEF) and the Hubble Space Telescope (HST) solar array (SA) multilayer insulation (MLI). All samples were supplied by the Materials Physics and Chemistry Section of ESA's European Space Research and Technology Center.

II. Experimental Part

A. Scanning Thermal Microscopy

The different polymer samples were inspected using SThM techniques and LTA to determine material differences that may occur due to space environmental ground simulation. Therefore, the samples were explored using the atomic force microscopy mode. The samples were scanned at two different places at temperatures of

Received 10 July 2007; revision received 18 June 2008; accepted for publication 18 June 2008.

*Materials Performance, P.O. Box 6235; Faculty of Aerospace Engineering, Fundamentals of Advanced Materials, Kluyverweg 1; hartmut.fischer@tno.nl.

†European Space Research and Technology Centre; Materials Physics and Chemistry Section, P.O. Box 299, Keplerlaan 1; Christopher.Semprimoschnig@esa.int.

200°C using a thermal probe to detect the surface profile and thermal diffusion profiles in an area of 100×100 μm. The results are presented in plots of the thermal and topological images of the samples.

B. Local Thermal Analysis

LTA was performed on 8 different places using a scanning speed of 5 K/s in a temperature range between 20 and 400°C; 20 data points were collected per second. The probes have a spring constant of about 10 N/m, resulting in a contact force of about 1 μm and a contact pressure of about 1 MPa. The contact surface area between probe and substrate (approximately 2–6 μm^2) was determined by inspection of the mark of the probe left on the substrate after a short contact on a polystyrene surface (1–2 s) at 100°C. Different contact forces ranging between 20 and 60 nN resulted in only small differences in the size of the penetration marks left behind when making contact at temperatures below T_g. Calibration of the thermal probe was performed following known procedures and using well-defined calibration samples for the detection of melting points and glass transition temperatures (see Table 1).

The samples under investigation are listed in Table 2. The test samples from the space environmental ground simulation were thermally aged silicone adhesive, Kapton HN, and Upilex S. The polyimides were coming from a test campaign reported in [4]. Seven samples of ground-tested FEP were investigated. Two were purely solar UV (SUV, 200–400 nm) irradiated, one was mostly vacuum UV (VUV, 115–200 nm) irradiated, one was UV irradiated and thermally aged, one was UV irradiated and thermally cycled, one was purely thermally aged, and one was purely thermally cycled. For the FEP samples, two reference materials were supplied; for the other three materials, one reference sample was supplied. In addition, four space-retrieved FEP material samples coming from the LDEF and the HST SA MLI. The LDEF samples came from rows 4 and 10, respectively; the HST SA MLI samples came from the primary deployment mechanism (PDM), of which one sample came from the solar-facing side and the other sample came from the antisolar side. All irradiated samples were analyzed from the top surface, which corresponds to the first impingement of radiation.

III. SThM Results of Aged and Exposed Silicones, Polyimides, and FEP

The silicones and the FEP sample surfaces show no signs of degradation using our methods either in topology or in mapping thermal conductivity. Kapton HN also shows no signs of degradation after exposure for 763 h at 350°C, whereas Upilex S shows an appearance of areas of lower thermal conductivity (holes) in the thermally treated material compared with the virgin material (see Fig. 1).

These features are especially well visible during scanning in the thermal mode and may be possible signs of either degradation, the formation of small shallow holes filled with air (and hence displaying a much lower heat conductivity), or perhaps cross-linking (also resulting in areas of lower heat conductivity). However, further investigations are needed to clarify the origin of these features in detail and the connected process during the thermal aging treatment.

Table 1 Samples used for the thermal calibration of the probe for the detection of melting temperatures and glass transition temperatures

Material trade name and type	Glass transition temperature T_g, °C	Melting temperature T_m, °C
Paraffin $C_{24}H_{30}$	——	48
Paraffin $C_{32}H_{66}$	——	70
Polyethylene oxide	——	63
Low-density polyethylene	——	124
High-density polyethylene	——	136
Isotactic polypropylene	——	163
Nylon (polyamide 6)	——	216
Mylar (polyethylene terephthalate)	——	266
Poly-3-methylbutene	——	305
Plexiglas (polymethyl methacrylate)	105	——
Polystyrene	105	——
Zeonex 480R (cyclic olefin polymer)	138	——
Topas 6013 (cyclic olefin copolymer)	140	——
Makrolon (poly carbonate)	150	——
Zeonor 1600 (cyclic olefin polymer)	163	——
Udel P3500 (polysulfone)	185	——

Table 2 Samples investigated within this study

Sample no. and material type	Treatment
Silicone, 1 mm	None, reference
Silicone, 1 mm	Thermal, 4430 h at 190°C
Kapton HN, 25 μm	None, reference
Kapton HN, 25 μm	Thermal, 763 h at 350°C
Upilex S, 25 μm	None, reference
Upilex S, 25 μm	Thermal, 763 h at 350°C
FEP, 127 μm	None, reference
FEP, 127 μm	Thermal, 44.8 days at 200°C
FEP, 127 μm	Thermal, 6354 cycles at $\pm$100°C
FEP, 1 mm	4110 ESH SUV, +6354 cycles at $\pm$100°C, 15 krad, Co 60
FEP, 127 μm	8740 ESH VUV.
FEP, 127 μm	HST, antisolar side, I1
FEP, 127 μm	HST, solar side, C1
FEP, 127 μm	LDEF, row 10, 69-month space 10,000 h, sun + ATOX
FEP, 127 μm	LDEF, row 4, 69-month space, 10,000 h, sun
FEP, 1 mm	None, reference
FEP, 1 mm	4110 ESH SUV

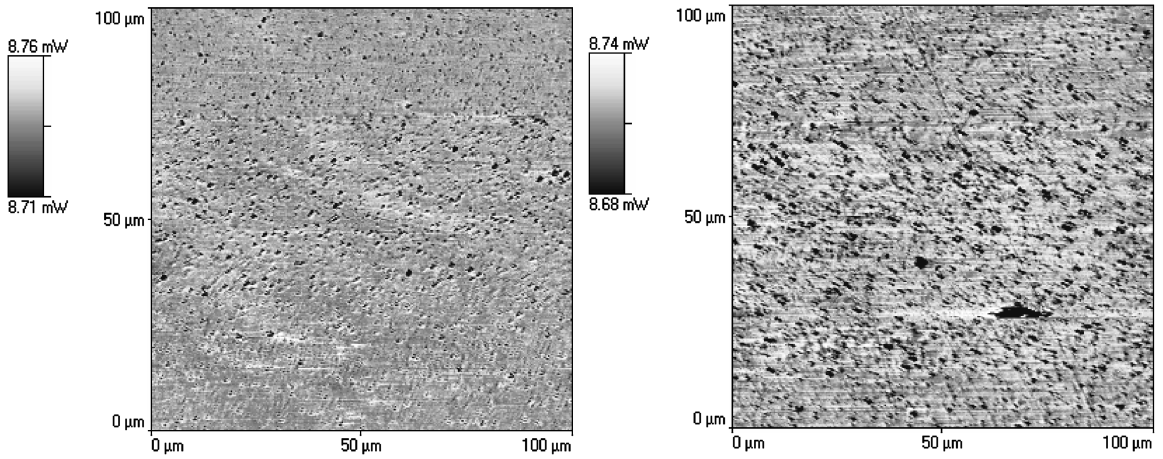

Fig. 1 Thermal images of Upilex S film scanned at 200°C before and after thermal aging. The thermally aged sample (right) shows larger thermal defects, hinting at partial thermal degradation of the surface.

IV. LTA Results of Aged and Exposed Silicones, Polyimides, and FEP

LTA on the silicone adhesive and the polyimides shows no differences in thermomechanical behavior between the reference samples and the thermally aged/exposed samples, because their main transitions are either too low or too high with respect to temperature. On the other side, a comparison of the thermomechanical signal of virgin and exposed/aged FEP instead shows distinct changes of the melting/softening behavior, depending on the treatment [increases in the coefficient of thermal expansion (CTE) and reduction of T_g and melt viscosity, etc.]. Both degradation and cross-linking were observed. It is shown that the method is particularly suitable for this material, and subtle differences of the top surface layer caused by different exposure conditions can be revealed. This will be discussed in detail subsequently.

Pure thermal treatment/aging for either 44.8 days at 200°C or for 6354 cycles changing between 100 and 100°C results only in a change in penetration depth but no change in CTE, position, or slope of the softening; thus, no degradation (see Fig. 2) can be found. Complementary experiments using conventional differential scanning calorimetry show an increase in degree of crystallinity; hence, the change in penetration depth may be related to this effect. This is not at all surprising, because of the fact that an analogous polymer, polytetrafluoroethylene, is thermally stable up to temperatures of 320°C.

SUV [4110 equivalent solar hours (ESH)], γ radiation (15 krad) exposed and thermally cycled samples, and SUV (4110 ESH) irradiated-only samples show a totally different behavior: the thermomechanical behavior is drastically changed (see Fig. 3). A dramatically decreased penetration of the sensor during heating coupled with a shift of the softening temperature to slightly larger temperatures (at around 310°C, T_m shifts upward by 10 K) is observable. Almost no penetration of the sensor occurred after softening. This hints to a cross-linking at the surface, which causes an increase in stiffness, especially of the rubbery phase. A subsequent or parallel thermal aging process (thermal cycling for 6354 cycles, ±100°C) has no additional effect. Also, no effect of the additional γ radiation (15 krad) was discernible.

VUV irradiation causes a slight decrease in the softening point (reduction of the softening temperature by about 15 K), hinting at a (partial) degradation of FEP under irradiation of shorter wavelength instead of cross-linking (see Fig. 4). This result is not at all surprising, because a degradation of FEP under VUV or soft x-ray irradiation is well known to the material scientists in the space community. Previous studies already revealed the formation of volatile C_nF_m species upon VUV and soft x-ray radiation of FEP connected with a C–C bond scission and an erosion of the polymer [5–11]. This also resulted in severe degradation of the mechanical properties.

The different results of the two ground-based irradiated samples may be explainable if the possible photolysis reactions occurring are more closely analyzed (see Fig. 5). The first, and possibly dominant, process is the abstraction of fluorine atoms (process a), which may be followed by two subsequent processes ($b1$ and $b2$). Obviously, differences in radiation energy cause different processes to occur preferentially; in the case of more energetic irradiation (VUV or soft x-rays), chain scission is obviously preferred, whereas longer wavelength irradiation leads to (surface) cross-linking (Fig. 5).

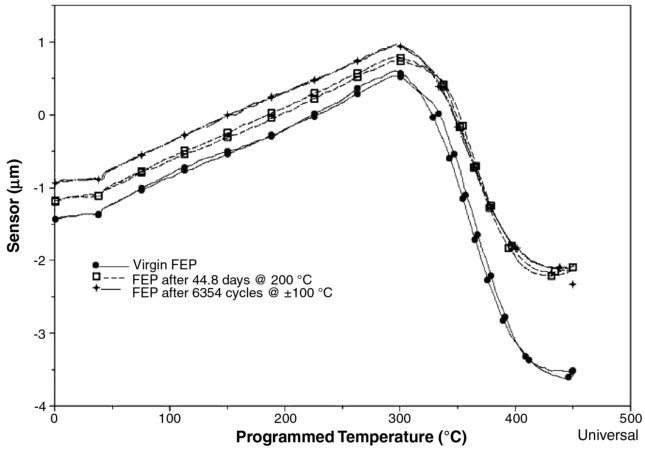

Fig. 2 Results of the LTA experiments performed on virgin and thermally aged FEP films. Thermal aging causes only a change in penetration depth but no changes otherwise (shift of transition temperature) and hence no signs of degradation.

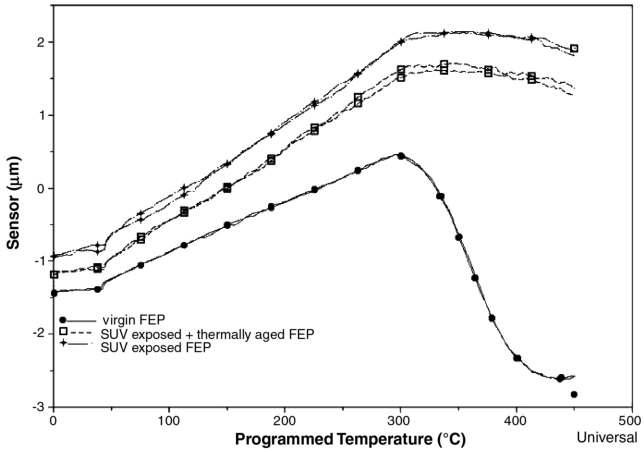

Fig. 3 Results of the LTA experiments performed on virgin and on SUV irradiated (and thermally aged) FEP films. SUV irradiation causes hardening of the film, especially at temperatures above T_m, hinting at cross-linking.

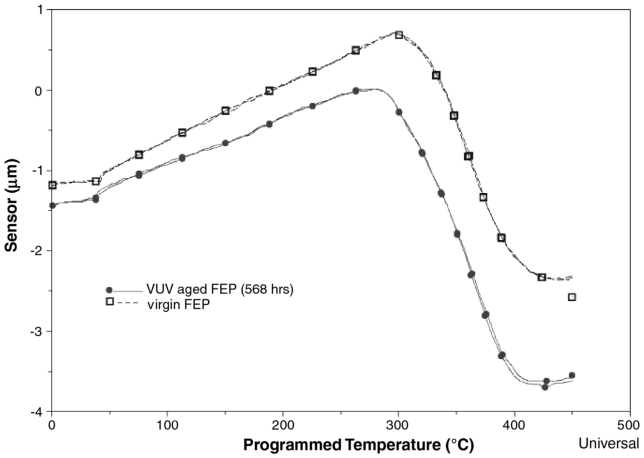

Fig. 4 Results of the LTA experiments performed on virgin and on VUV irradiated FEP films. VUV irradiation causes (in contrast to the SUV) irradiation degradation connected with chain scission and no cross-linking.

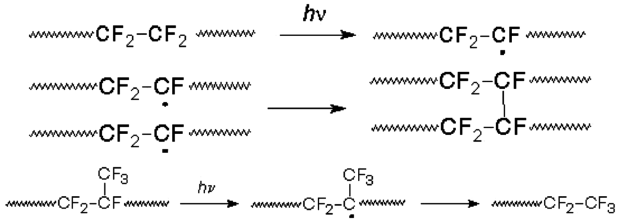

Fig. 5 Scheme 1: possible FEP degradation mechanism upon UV irradiation.

V. Results on Space-Retrieved Samples

Two sets of samples obtained from space environmentally exposed samples were also inspected. One set was retrieved from the HST SA PDM MLI. One sample came from the antisolar side (I1) and one came from the solar side (C1). The HST SA MLI materials have been already part of extensive analysis and investigations. It is well established that FEP used as a second surface mirror tends to degrade, and mechanical degradation and cracking have been observed in space as well as on the ground after retrieval. Also, on the retrieved material from that part of the HST, degradation has been found in other work [12–15]. An image of the space-retrieved blanket is shown in Fig. 6.

The antisolar-side exposed sample (I1) shows an increase in melting temperature, either based on cross-linking due to irradiation or explainable by a deposited silica top layer as measured by x-ray photoelectron spectroscopy (XPS) [16].

This is in agreement with the increase in elastic modulus as measured macroscopically. The solar side (C1) shows clear signs of degradation, as expressed by a decrease in melting/softening temperature, together with a drastic decrease in melt viscosity, seen as a change in the slope of penetration after crossing over the melting temperature (see Fig. 7). Again, this is in agreement with macroscopic tensile testing experiments in which severe embrittlement has been found coupled with an increase in the degree of crystallinity, which has been attributed to the formation of short-chain fluorocarbons, which are able to crystallize more efficiently [17].

Additional topological studies were carried out using standard Si_3N_4 probes (nominal tip radius of 20 nm) in contact mode and soft Si tips (nominal tip radius of 15–20 nm) in noncontact mode as well as supersharp Si tips (nominal tip radius of 5–10 nm) in noncontact mode. Depending on the position of the sample retrieval from the FEP film, different types of topology are observable. The samples taken from areas C, D, and (partially) E indicated in Fig. 6 show surfaces that appear eroded and have a conelike or carpet-type morphology, as depicted in Fig. 8. This characteristic is typical of directed atomic oxygen (ATOX) erosion on materials that produce gaseous oxidation. This phenomenon drastically reduces ultraviolet, visible, and infrared transmissions. The features of the surface are comparable with another photograph obtained by NASA showing ATOX exposure of a Kapton sample onboard the LDEF facility [18,19].

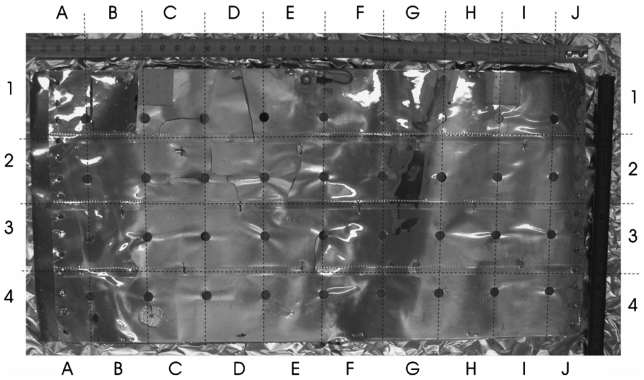

Fig. 6 Photograph of the irradiated FEP film as retrieved from HST. The samples under investigation were taken from areas C1 (solar side) and I1 (antisolar side).

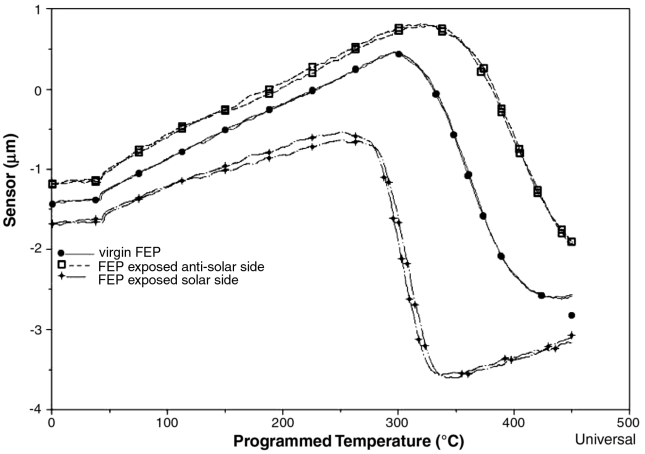

Fig. 7 Results of the LTA experiments performed on the FEP samples retrieved from the HST. Both samples show signs of degradation via chain scission; the more severe degradation was observed for the sample originating from the solar-side sample.

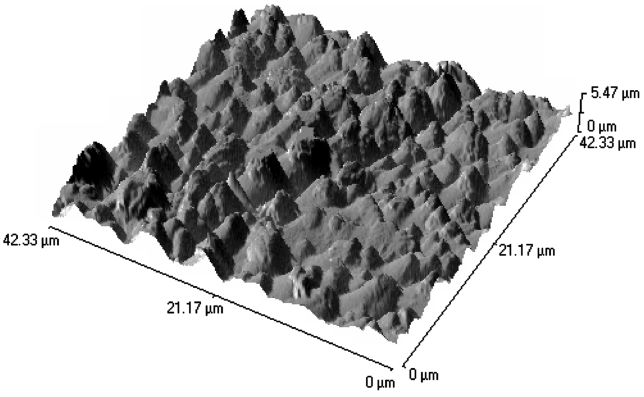

Fig. 8 Typical LEO erosion features of sample from area D; conical structures with dimensions of several microns and depths of 5–10 μm are as expected, because this area was heavily exposed to ATOX and VUV. The sample also shows a significantly different appearance: the originally transparent/translucent FEP has turned white due to the diffuse diffraction of light on the surface caused by the changed surface structure.

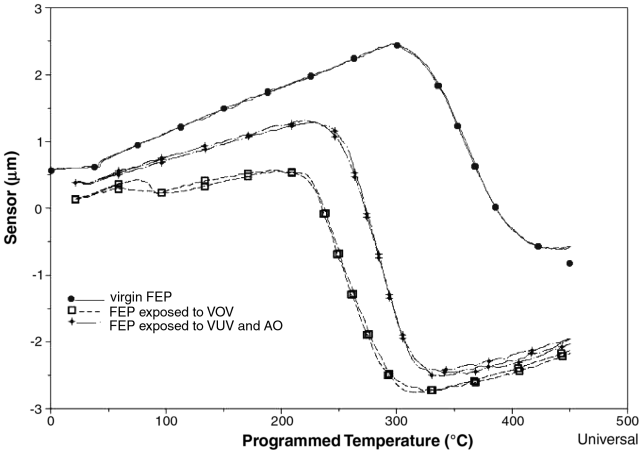

Fig. 9 Results of the LTA experiments performed on virgin FEP and on the samples retrieved from the LDEF. Both samples show clear signs of degradation via chain scission; the sample not exposed to ATOX even has a deposit of short-chain fluorocarbons with a distinct melting point of about 80°C.

On the other side, the antisolar side was retrieved from an area that was only exposed to less VUV as well as ATOX. The erosion structure is very different from structures originated by exposure to higher levels of ATOX and VUV. The few cones visible may be artifacts, and the structure in the middle is a more typical increased porosity of the surface. It may well be that a small surface contamination, as noticed in [16], leads to a protection of the outer layers.

A second set of space-retrieved samples was analyzed that came from the LDEF. This facility, which was in a low-Earth-orbit (LEO) environment for 69 months between 1984 and 1990, has been the subject of extensive postretrieval analysis. For details, the reader is referred to [20,21], for instance.

One sample came from row 4, which was mostly sun-exposed (UV, VUV, x-ray, etc.), with hardly any ATOX, and the other one came from row 10, which was beside the sun exposure also in the direction of ATOX exposure.

It is known that exposure of FEP to ATOX and VUV results in erosion of the polymer, just as with exposure to VUV. Although only a little oxygen absorption is detectable after atomic oxygen exposure, it was concluded that in this case, the degradation also occurred via C–C bond scission under transient direct action of ATOX.

The sample with the combined exposure (VUV and ATOX) shows only a slight degradation (a reduction of the T_m by about 10 K), whereas the sample, which was only exposed to VUV, shows signs of a more severe degradation: a reduction of the T_m by about 35 K (see Fig. 9). The thermomechanical behavior also indicates the presence of rather short C_nF_m species close to the surface: a 150–250-nm-thick layer material with a very low T_m (~80°C).

These observations fit very well with previous findings that revealed severe mechanical embrittlement of samples from row 4 but less mechanical embrittlement of samples of row 10 [5,11]. The erosion caused by the combined action of hard radiation (VUV, etc.) and ATOX might actually elevate the surface embrittlement. It has also been suggested in the past that the severe degradation of row 4 was caused by solar flares [7]. This would fit well with the observed results on the ground-tested samples of this work. In the case of row 10, however, the impact and reaction with ATOX may cause the chain-scission-formed short chains to fragment more efficiently than the long chains, and hence the remaining material will appear to be less degraded. However, the total mass loss should also be taken into account, which is higher in the case of the combined action of VUV and ATOX and hence supports our interpretation.

VI. Conclusions

Fluoropolymers are widely used for space applications such as radiator materials or electrical wire insulators. They generally show a better resistance to ATOX than hydrocarbon-based polymers; the reaction efficiency of Teflon fluorinated ethylene propylene (FEP) is less than 0.05×10^{-24} cm^3/O atom, compared with 3×10^{-24} cm^3/O atom for Kapton [18]. Fluoropolymers are more sensitive to ATOX than to VUV radiation and the dominant erosion mechanism is scission. A combination of ATOX and VUV is by far more severe than both factors separately; the erosion can be determined in terms of mass loss and increased surface roughness. The extreme temperatures of the space environment also reduce the lifetime of fluorine-based polymers in space.

In this work, a new method, the scanning thermal microscopy method, was applied to study the durability of polymeric materials for space applications. Samples were analyzed by the scanning mode and particularly by the local thermal analysis mode.

The method was applied to study ground-tested as well as space-retrieved materials. As materials, space-grade silicones, high-temperature polyimides, and the well-known second-surface-mirror-material FEP were analyzed.

It was shown that the method is particularly suitable for the FEP material, and subtle differences of the top surface layer caused by different exposure conditions can be revealed. It was found that thermal treatment (aging or cycling) leads to a change in the penetration depth of the surface sensor and is possibly caused by an increase of crystallinity. SUV irradiation leads to a surface cross-linking (revealed by a drastically decreased penetration and a shift of T_m to higher temperatures). VUV radiation leads to chain scission (revealed by a shift of the T_m to lower temperatures and a decrease of melt viscosity).

Clear degradation of space-retrieved materials from both the HST SA PDM MLI and the LDEF MLI was revealed. Obtained results fit very well with previously (macroscopically) observed results such as the embrittlement of row 4 of the LDEF MLI. Direct sun exposure leads (by combined action of VUV and ATOX) to severe degradation of the FEP surface: a conical structure was observed, coupled with a decrease in melting point and increase in penetration speed, which is coupled with an decrease in molecular weight. The opposite was observed for the sample retrieved from the antisolar side: an increase in melting point and melt stiffness was observable, most likely coupled with the cross-linking reaction and/or deposition of silicon at the surface.

Overall, it was shown that the technique proves to be very suitable for the study of the surface-degradation effects of materials exposed to space as well as to a simulated space environment. The obtained results fit very well with previously (macroscopically) observed results.

Acknowledgments

The support of S. Heltzel, F. Prins, and E. F. Lisbona for the space-simulated ground tests at the European Space Research and Technology Center is gratefully acknowledged. The support of ESA is under contract.

References

[1] Price, D. M., Reading, M., Caswell, A., Hammiche, A., and Pollock, H. M., "Micro-Thermal Analysis: A New Form of Analytical Microscopy," *Microscopy and Analysis*, Vol. 65, 1998, pp. 17–19.

[2] Hammiche, A., Hourston, D. J., Pollock, H. M., Reading, M., and Song, M., "Scanning Thermal Microscopy: Subsurface Imaging, Thermal Mapping of Polymer Blends, and Localized Calorimetry," *Journal of Vacuum Science and Technology B (Microelectronics and Nanometer Structures)*, Vol. 14, No. 2, 1996, pp. 1486–1491. doi:10.1116/1.589124

[3] Hammiche, A., Bozec, L., Conroy, M., Pollock, H. M., Mills, G., Weaver, J. M. R., Price, D. M., Reading, M., Hourston, D. J., and Song, M., "Highly Localized Thermal, Mechanical, and Spectroscopic Characterization of Polymers Using Miniaturized Thermal Probes," *Journal of Vacuum Science and Technology B (Microelectronics and Nanometer Structures)*, Vol. 18, No. 3, 2000, pp. 1322–1332. doi:10.1116/1.591381

[4] Semprimoschnig, C. O. A., Heltzel, S., Eesbeek, M. v., Polsak, A., "Assessing The Limits Of Commercially Available Polyimides," *First*

European Workshop on Inflatable Structures, ESA WPP 2002, ESA, Noordwijk, The Netherlands, 2002, pp. 171–181.

[5] Van Eesbeek, M., Levadou, F., and Milintchouk, A., "A Study of FEP Behaviour in Space Environment," 25th International Conference on Environmental Systems, Society of Automotive Engineers Paper 951640, San Diego, CA, 1995.

[6] Van Eesbeek, M., Levadou, F., and Milintchouk, A., "Investigation on FEP from PDM and Harness from HST-SA1," *Hubble Space Telescope Solar Array Workshop Proceedings (WPP—77)*, European Space Technology and Research Centre, Noordwijk The Netherlands, 1995, pp. 403–416.

[7] Milintchouk, A., Van Eesbeek, M., Levadou, F., and Harper, T., "Influence of X-Ray Solar Flare Radiation on Degradation of Teflon in Space," *Journal of Spacecraft and Rockets*, Vol. 4, No. 34, 1997, pp. 542–548.

[8] Van Eesbeek, M., Levadou, F., Tupikov, V. I., Cherniavsky, A. I., Khatipov S. A., Milinchuk, V. K., Stepanov V. F., and Milintchouk A. V., "Degradation of Teflon PTFE and FEP Exposed to Far Ultraviolet Radiation," *Sixth International Symposium on Materials in a Space Environment*, ESA-SP368, ESA, Noordwijk, The Netherlands, 1994, pp. 149–164.

[9] Dever J. A., and McCracken, C. A., "Effects of Vacuum Ultraviolet Radiation of Various Wavelength Ranges on Teflon FEP Film," *High Performance Polymers*, Vol. 16, No. 2, 2004, pp. 289–301. doi:10.1177/0954008304044099

[10] Weihs, B., and van Eesbeek, M., "Secondary VUV Erosion Effects on Polymers in the ATOX Atomic Oxygen Exposure Facility," *Sixth International Symposium on Materials in a Space Environment*, ESA-SP368, ESA, Noordwijk NL, 1994, pp. 277–283.

[11] Skurat, V. E., Samsonov, P. V., and Nikiforov, A. P., "Vacuum Ultraviolet Radiation in Sources of Hyperthermal Atomic Oxygen. Photodestruction of Polytetrafluoroethylene (PTFE) and Teflon FEP for Indication of This Radiation," *High Performance Polymers*, Vol. 16, No. 2, 2004, p. 339. doi:10.1177/0954008304044104

[12] Dever, J. A., de Groh, K. K., Banks, B. A., Townsend, J. A., Barth, J. L., Thomson, S., Gregory, T., and Savage, W., "Environmental Exposure Conditions for Teflon Fluorinated Ethylene Propylene on the Hubble Space Telescope," *High Performance Polymers*, Vol. 12, No. 1, 2000, pp. 125–139. doi:10.1088/0954-0083/12/1/310

[13] Zuby, T. M., de Groh, K. K., and Smith, D. C., "Degradation of FEP Thermal Control Material Returned from the Hubble Space Telescope," *Hubble Space Telescope Solar Array Workshop Proceedings (WPP—77)*, European Space Technology and Research Centre, Noordwijk, The Netherlands, 1995, pp. 385–402.

[14] De Groh, K. K., Dever, J. A., Sutter, J. K., Gaier, J. R., Gummow, J. D., Scheiman, D. A., and He, C., "Thermal Contributions to the Degradation of Teflon FEP on the Hubble Space Telescope," *High Performance Polymers*, Vol. 13, No. 3, 2001, pp. S401–S420. doi:10.1088/0954-0083/13/3/332

[15] Moser, M., Semprimoschnig, C. O. A., van Eesbeek, M. R. J., Pippan R., "Comparison Of Results From Post Flight Investigation on FEP Retrieved from the Hubble Space Telescope Solar Arrays and LDEF," *Proceedings of the European Conference on Spacecraft Structures, Materials and Mechanical Testing* [CD-ROM], ESA SP 581, ESA, Noordwijk, The Netherlands, Sept. 2005.

[16] Moser, M., Semprimoschnig, C. O. A., and van Eesbeek, M. R. J., "Materials Analysis of Space Retrieved Materials from the Hubble Space Telescope," *10th ISMSE* [CD-ROM], ESA SP 616, ESA, Noordwijk, The Netherlands, Sept. 2006

[17] Lotz, B., "Phase Transitions and Structure of Crystalline Polymers," *Crystallisation of Polymers*, edited by M. Dosière, NATO ASI Series. Series C, Mathematical and Physical Sciences, Vol. 405, Kluwer Academic, Norwell, MA, 1993.

[18] Dooling, D., and Finckenor, M. M., "Material Selection Guidelines to Limit Atomic Oxygen Effects on Spacecraft Surfaces," NASA TP 209260, 1999.

[19] Grossman, E., and Gouzman, I., "Space Environment Effects on Polymers in Low Earth Orbit," *Nuclear Instruments and Methods in Physics Research. Section B: Beam Interactions with Materials and Atoms*, Vol. 208, Nos. 1–4, 2003, p. 48. doi:10.1016/S0168-583X(03)00640-2

[20] Levadou, F., and Pippin G., "Effects of the LDEF Environment on the Ag/FEP Thermal Blankets," *LDEF Materials Workshop '91*, NASA Langley Research Center, Hampton, VA, 1991, pp. 311–344.

[21] O'Neal, R., and Lightner E. B., "Long Duration Exposure Facility—A General Overview: LDEF, 69 Months in Space," *First Post-Retrieval Symposium*, NASA CP 3134, 1991, pp. 3–14.

J. Minow
Associate Editor